JVI Journals.ASM.org

Infection of Pericytes *In Vitro* by Japanese Encephalitis Virus Disrupts the Integrity of the Endothelial Barrier

Chun-Jung Chen,[a,b,c,d] Yen-Chuan Ou,[e] Jian-Ri Li,[e] Cheng-Yi Chang,[f] Hung-Chuan Pan,[g] Ching-Yi Lai,[a] Su-Lan Liao,[a] Shue-Ling Raung,[a] Chen-Jung Chang[h]

Department of Education and Research[a] Division of Urology,[e] and Department of Neurosurgery,[g] Taichung Veterans General Hospital, Taichung, Taiwan; Center for General Education, Tunghai University, Taichung, Taiwan[b]; Institute of Biomedical Sciences, National Chung Hsing University, Taichung, Taiwan[c]; Graduate School of Nursing, HungKuang University, Taichung, Taiwan[d]; Department of Surgery, Fong-Yuan Hospital, Taichung, Taiwan[f]; Department of Medical Imaging and Radiological Sciences, Central Taiwan University of Sciences and Technology, Taichung, Taiwan[h]

Though the compromised blood-brain barrier (BBB) is a pathological hallmark of Japanese encephalitis-associated neurological sequelae, the underlying mechanisms and the specific cell types involved are not understood. BBB characteristics are induced and maintained by cross talk between brain microvascular endothelial cells and neighboring elements of the neurovascular unit. In this study, we show a potential mechanism of disruption of endothelial barrier integrity during the course of Japanese encephalitis virus (JEV) infection through the activation of neighboring pericytes. We found that cultured brain pericytes were susceptible to JEV infection but were without signs of remarkable cytotoxicity. JEV-infected pericytes were found to release biologically active molecules which activated ubiquitin proteasome, degraded zonula occludens-1 (ZO-1), and disrupted endothelial barrier integrity in cultured brain microvascular endothelial cells. Infection of pericytes with JEV was found to elicit elevated production of interleukin-6 (IL-6), which contributed to the aforementioned endothelial changes. We further demonstrated that ubiquitin-protein ligase E3 component *n*-recognin-1 (Ubr 1) was a key upstream regulator which caused proteasomal degradation of ZO-1 downstream of IL-6 signaling. During JEV central nervous system trafficking, endothelial cells rather than pericytes are directly exposed to cell-free viruses in the peripheral bloodstream. Therefore, the results of this study suggest that subsequent to primary infection of endothelial cells, JEV infection of pericytes might contribute to the initiation and/or augmentation of Japanese encephalitis-associated BBB breakdown in concerted action with other unidentified barrier disrupting factors.

The blood-brain barrier (BBB) acts as an interface between the central nervous system (CNS) and the systemic compartments of the body and is a unique diffusion barrier which plays an important role in the maintenance of CNS homeostasis by restricting immune cell migration and diffusion of soluble molecules from the blood to the brain parenchyma. Endothelial cells in the brain microvasculature line the intraluminal portion of brain capillaries closely interconnected by continuous tight junctions and represent the cellular basis of the structural and functional integrity of the BBB. In addition to brain microvascular endothelial cells, the neurovascular unit of the BBB is also composed of the capillary basement membrane, neurons, astrocytic end-feet ensheathing the vessels, and pericytes embedded within the basement membrane. Brain microvascular endothelial cells have a dynamic interaction with those neighboring cells. The cross talk between the cells of the neurovascular unit and their cooperation are crucial for the formation of complex tight junctions and the maintenance of functional barrier integrity (1, 2).

The disruption of BBB integrity is a feature of several acute and chronic neurological disorders and plays a critical role in disease progression, including viral pathogenesis. Neurotropic virus-associated neuropathy is characterized by the presence of infectious virus particles, immune cells, inflammatory mediators, and eventual neuronal dysfunction or destruction in the parenchymal tissues of the CNS. Generally, BBB integrity is compromised during infection, and this BBB disruption dictates the aforementioned alterations and brain injury in several neurotropic viruses (3–6). Though most studies demonstrated the detrimental consequences of BBB breakdown during neurotropic virus infection, the opening of the BBB also prevents certain lethal viral CNS infections (7). Currently, the mechanisms of BBB disruption during neurotropic virus-associated pathologies are not fully understood.

Japanese encephalitis virus (JEV), an enveloped, single-stranded, positive-sense, neurotropic flavivirus, is an important human pathogen transmitted by the mosquito and may cause severe, even lethal, encephalitis (8, 9). Neurological complications such as inflammation and neuronal death contribute to the mortality and morbidity associated with JEV-induced encephalitis, and a high proportion of survivors have serious neurological and psychiatric sequelae (10, 11). During the course of JEV infection, the neuronal death rate and the mortality rate increase in patients with elevated levels of inflammatory mediators in the serum and cerebrospinal fluid (12, 13). The increased production of inflammatory mediators is also associated with high virus titers in the brain and increased mortality in Japanese encephalitis animal models (10, 11, 14). Although the exact mechanisms of neurotropic virus-associated CNS invasion and encephalitis are yet to be clearly defined, increasing evidence suggests the crucial role of the BBB in controlling viral entry and immune cell infiltration into the nervous tissues. Several clinical and experimental studies demonstrated the dysfunction and/or disruption of the BBB in

Received 24 September 2013 **Accepted** 2 November 2013
Published ahead of print 6 November 2013
Address correspondence to Chun-Jung Chen, cjchen@vghtc.gov.tw.

doi:10.1128/JVI.02738-13

Japanese encephalitis subjects, and these alterations were positively correlated with the severity of encephalitis (10, 15–18).

Since BBB endothelial cells are directly exposed to cell-free viruses in the peripheral bloodstream, they are highly expected to play a determinant role in neurotropic virus-associated BBB disruption. This hypothesis is supported by the finding that direct infection of BBB endothelial cells with Semiliki Forest virus caused disruption of endothelial barrier integrity (6). Further evidence has demonstrated that the BBB is not intrinsic to the endothelial cells but is regulated by interactions with neighboring cells. Brain pericytes, the nearest neighbors of brain microvascular endothelial cells sharing a common basal membrane in cerebral capillaries, have a regulatory effect on BBB integrity (19–21). Virus-infected or stressed pericytes produced elevated levels of proinflammatory cytokines and compromised the integrity of the BBB *in vitro* (22–24). Although the viruses can be detected in BBB endothelial cells after systemic infection (17), the results of a brain microvascular endothelial cell monoculture model study showed that the increased vascular permeability during JEV infection could not solely be produced by endothelial infection (25). The mechanisms of BBB disruption during JEV-associated pathologies are not fully understood. To extend the scope of understanding of cellular mechanisms associated with JEV-induced BBB disruption, our aim was to study the impact of pericytes on the barrier properties of brain microvascular endothelial cells during the course of JEV infection. We found that JEV infection resulted in compromised integrity of an *in vitro* BBB model coculturing of brain microvascular endothelial cells and pericytes. Soluble bioactive interleukin-6 (IL-6) derived from JEV-infected pericytes contributed to endothelial zonula occludens-1 (ZO-1) degradation, leading to barrier disruption. These endothelial changes were accompanied by activation of IL-6-induced ubiquitin-proteasome-dependent degradation machinery.

MATERIALS AND METHODS

Virus. JEV NT113 was propagated in C6/36 cells (BCRC-60114; Bioresource Collection and Research Center, Hsinchu, Taiwan) utilizing Dulbecco's modified Eagle medium (DMEM) containing 5% fetal bovine serum (FBS). For virus inactivation, JEV stocks were incubated at 94°C for 15 min (JEV/heat inactivated). Baby hamster kidney cells (BHK21, BCRC-60041; Bioresource Collection and Research Center, Hsinchu, Taiwan) were used to determine viral titers. To conduct viral infection, cells were adsorbed with JEV for 1 h at 37°C as described in our previous report (25). After adsorption, the unbound viruses were removed by gentle washing with phosphate-buffered saline (PBS). Fresh medium was added to each plate for further incubation at 37°C.

Brain microvascular endothelial cells and pericytes. The protocol for this animal study was approved by the Animal Experimental Committee of Taichung Veterans General Hospital. Brain microvascular endothelial cells and pericytes were isolated from adult female Sprague-Dawley rats (BioLASCO Taiwan Co., Ltd.) and cultured according to previously reported methods with some modifications (26). Briefly, the gray matter was minced and digested for 2 h at 37°C with 1 mg/ml of collagenase in DMEM. The cell pellets were separated by centrifugation for 20 min at 1,000 × *g* in 20% bovine serum albumin in DMEM. The microvessels obtained in the pellets were digested further with 1 mg/ml of collagenase-dispase in DMEM for 1.5 h at 37°C. The digested microvessel solution was centrifuged at 700 × *g* and 4°C for 6 min. Percoll was mixed in a 9:1 ratio with 10×-concentrated PBS. This solution was diluted 1:3 in PBS containing 5% FBS. The mixture was sterilized using a 0.2-μm syringe filter and centrifuged in a fixed-angle rotor for 60 min at 30,000 × *g* and 4°C for Percoll gradient formation. The pellets were resuspended and layered over a 33% continuous Percoll gradient and centrifuged at 1,000 × *g* for 10 min at 4°C. Subsequently, the microvessel layer was removed and diluted into DMEM. After centrifugation at 700 × *g* for 10 min, cell pellets were resuspended and used for cultivation. For pericyte preparation, the obtained cells were seeded onto uncoated dishes and cultured in DMEM containing 10% FBS for 10 days. For endothelial cells, another set of cells were seeded onto collagen-coated dishes. Cells were cultured in DMEM containing 20% horse serum, 40 μg/ml of endothelial cell growth supplements, and 4 μg/ml of puromycin. Two days after the initial plating, cells were fed with culture medium without puromycin and fed every 2 days afterwards (7 to 10 days). The resultant cells were microvascular endothelial cells. To measure the integrity of the endothelial barrier, brain microvascular endothelial cells (1×10^5) were seeded onto collagen-coated Transwell filter inserts (24-well; BD, San Jose, CA) 3 days prior to experiments. Two experimental conditions were designed to establish the coculture system. Brain microvascular endothelial cells (9×10^4) were first seeded onto collagen-coated Transwell filter inserts. Twenty-four hours later, pericytes (1×10^4) were seeded onto the same Transwell filter inserts grown with monolayers of brain microvascular endothelial cells. These cocultured cells were used two additional days later. In another set, brain microvascular endothelial cells (9×10^4) and pericytes (1×10^4) were seeded onto collagen-coated Transwell filter inserts and 24-well plates, respectively. Three days later, the coculture was constructed by putting Transwell filter inserts into 24-well plates and was then used for experiments.

Cell viability assessment. [3-(4,5-Dimethylthiazol-2-yl)-5-(3-carboxymethoxyphenyl)-2-(4-sulfophenyl)-2H-tetrazolium] (MTS; Promega, Madison, WI) assay was performed to measure cell viability in a 96-well plate according to the manufacturer's instructions.

Immunofluorescence staining. The cells were washed twice with PBS, fixed with 4% paraformaldehyde in phosphate buffer (PB; 0.1 M Na_2HPO_4 and 0.1 M NaH_2PO_4) for 10 min, permeabilized with 0.1% Triton X-100 for 15 min, and washed with PBS. The cells were blocked with 5% nonfat milk in PBS for 30 min and then incubated with antibody against occludin (Santa Cruz Biotechnology, Santa Cruz, CA) or zonula occludens-1 (ZO-1, Invitrogen, Carlsbad, CA) overnight at 4°C, followed by washing with PBS. After washing, the cells were incubated with rhodamine- or fluorescein isothiocyanate (FITC)-conjugated secondary antibody for 1 h at room temperature. The nuclei were counterstained with Hoechst 33342. The fluorescent signals were observed under a fluorescence microscope.

Flow cytometry measurement. For the detection of CD31-positive cells, the detached cells were washed in PBS and stained with monoclonal antibody against CD31 (GeneTex, Irvine, CA). Antibody-labeled cells were washed and fixed in PBS with 0.37% formaldehyde. To identify cells expressing α-smooth muscle actin (α-SMA), the cells were then incubated with permeabilization buffer (0.5% saponin, 0.005% Tween 20, 0.2% FBS, and 0.1% NaN_3 in PBS), stained with anti-α-SMA antibody (Dako, Carpinteria, CA), washed in PBS, and resuspended in PBS-formaldehyde. These cells were then incubated with FITC-conjugated secondary antibody. Characterization of antibody-labeled cells was performed on a BD FACScalibur flow cytometer.

Western blot analysis. Cells were washed twice with PBS and harvested in Laemmli SDS sample buffer. Protein extracts were separated by SDS-PAGE and electrophoretically transferred to polyvinylidene difluoride membranes. After blocking, the membranes were incubated with antibodies against the following: ZO-1 (Invitrogen, Carlsbad, CA), ZO-2, occludin, claudin-1, claudin-5, ubiquitin-protein ligase E3 component, *n*-recognin-1 (Ubr 1; Santa Cruz Biotechnology, Santa Cruz, CA), JEV NS3, and β-tubulin (BD, San Diego, CA). After washing, a 1:10,000 (vol/vol) dilution of horseradish peroxidase-labeled IgG was added at room temperature for 1 h. Finally, the blots were developed using enhanced chemiluminescence Western blotting reagents. The intensity of each signal was determined by a computer image analysis system (IS1000; Alpha Innotech Corporation).

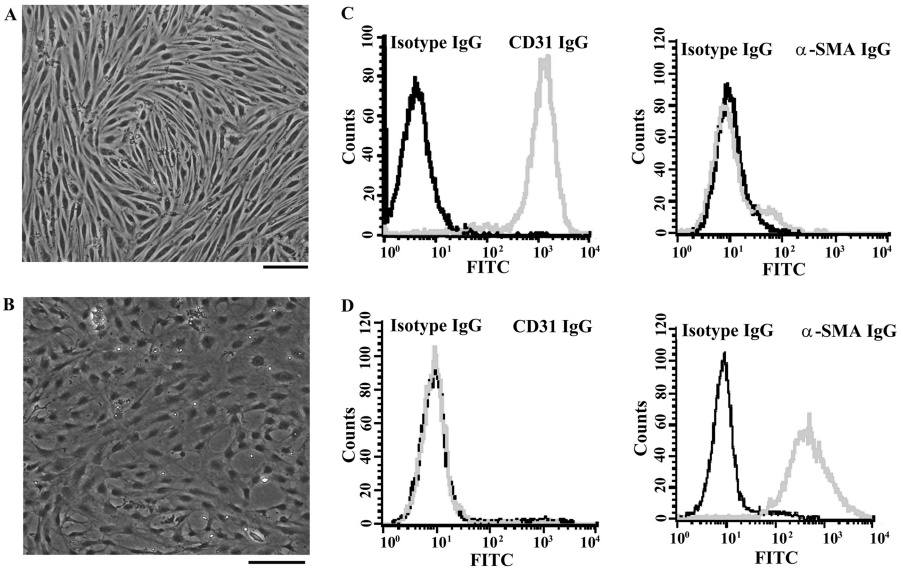

FIG 1 Characterization of cultured brain microvascular endothelial cells and pericytes. Confluent monolayers of brain microvascular endothelial cells (A) and pericytes (B) were observed under a light microscope. Scale bar = 50 μm. The dissociated brain microvascular endothelial cells (C) and pericytes (D) were subjected to immunofluorescence staining with isotype IgG and IgG against CD31 or α-SMA. Characterization of antibody-labeled cells was performed on a BD FACScalibur flow cytometer.

TEER. The culture medium was aspirated and then washed three times with medium. After the insert was dropped into medium, the barrier function of the endothelial monolayer was estimated by measuring the transendothelial electrical resistance (TEER) with a Millicell ERS ohmmeter (Millipore, Billerica, MA), as previously reported (27). The values were corrected for the background resistance measured across the filter without cells.

Transendothelial permeability assay. Transendothelial permeability assay was carried out according to previously reported methods, with some modifications (28). Brain microvascular endothelial cells were grown on 3-μm-pore Transwell filter inserts until confluent. After treatments, dextran-FITC was applied apically at 0.1 μg/ml for 30 min. Samples were removed from the lower chamber for fluorescence measurements and compared to control monolayers. Fluorescence was measured using a fluorometer (E_x 492 nm and E_m 520 nm, where E_x is excitation wavelength and E_m is emission wavelength).

RNA isolation and quantitative real-time RT-PCR. Total cellular RNAs were extracted from the cells using a TRIzol RNA isolation reagent (Invitrogen, Carlsbad, CA) and subjected to cDNA synthesis using random primers and Moloney murine leukemia virus (MMLV) reverse transcriptase (Epicentre Biotechnologies, Madison, WI). Quantitative real-time reverse transcriptase PCR (RT-PCR) was performed on ABI StepOne (Applied Biosystems, Foster City, CA), as previously reported (29). Relative gene expression was determined by the threshold cycle ($\Delta\Delta C_T$) method. Primers used for amplifications were as follows: ZO-1, 5′-CAGGTCTCTGTCACGCTTCT and 5′-AGTATTCATGGAAGGGAATA; JEV, 5′-AGAGCACCAAGGGAATGAAATAGT and 5′-AATAGGTTGTAGTTGGGCACTCTG; and β-actin, 5′-AAGTCCCTCACCCTCCCAAAAG and 5′-AAGCAATGCTGTCACCTTCCC.

ELISA. The levels of tumor necrosis factor alpha (TNF-α), interleukin-1β (IL-1β), IL-6, and vascular endothelial growth factor (VEGF) in the supernatants were measured using an enzyme-linked immunosorbent assay (ELISA) kit according to the manufacturer's instructions (R&D Systems, Minneapolis, MN).

siRNA transfection. The Ubr 1 and control small interfering RNAs (siRNAs) were purchased from Santa Cruz Biotechnology (Santa Cruz, CA). Microvascular endothelial cells were transfected with siRNAs using INTERFERin siRNA transfection reagent (Polyplus Transfection Inc., New York, NY) according to the manufacturer's instructions. The resultant cells were used 4 h after transfection.

Proteasome activity assay. After treatment, cells were homogenized on ice in a lysis buffer containing 50 mM Tris-HCl (pH 7.4), 5 mM $MgCl_2$, and 250 mM sucrose. The homogenates were centrifuged at 10,000 × *g* for 20 min at 4°C, and the resultant supernatants were recentrifuged at 100,000 × *g* for 1 h at 4°C. The final pellet, containing proteasomes, was resuspended in buffer containing 50 mM Tris-HCl (pH 7.4), 5 mM $MgCl_2$, and 20% glycerol. The MG132-inhibitable proteasome activity was measured by incubating the supernatants in reaction buffer containing 50 mM Tris-HCl (pH 8.0), 10 mM $MgCl_2$, 1 mM 1,4-dithiothreitol (1,4-DTT), and fluorogenic peptide substrates Suc-LLVY-AMC (chymotrypsin-like activity) or Suc-LLE-AMC (trypsin-like activity) (Calbiochem, San Diego, CA) for 45 min at 37°C. The levels of released AMC moiety were measured at an excitation of 380 nm and an emission of 460 nm. The arbitrary unit was expressed as the fluorescence change per amount of protein.

Caspase-3 activity assay. After treatment, cells were homogenized on ice in a lysis buffer containing 20 mM HEPES (pH 7.4), 4 mM EDTA, 1 mM EGTA, 5 mM $MgCl_2$, and 1 mM DTT. An aliquot of 50 μl of supernatant was incubated with an equal volume of the reaction buffer containing 20 mM HEPES (pH 7.4), 4 mM EDTA, 0.2% 3-[(3-cholamidopropyl)-dimethylammonio]-1-propanesulfonate (CHAPS), 10 mM DTT, and caspase-3-specific fluorogenic peptide substrates (BioVision, Mountain View, CA). The levels of released AMC moiety were measured at an excitation of 380 nm and an emission of 460 nm. The arbitrary unit was expressed as the fluorescence change per amount of protein.

Gelatinase zymography. Supernatants (15 μl) were assayed for gelatinase activity by zymography and underwent electrophoresis in polyacrylamide gels containing 0.5 mg/ml of gelatin in the presence of SDS under nonreducing conditions. After electrophoresis, the gels were washed twice in 2.5% Triton X-100 for 1 h, rinsed briefly, and incubated at 37°C for 24 h in 100 mM Tris-HCl (pH 7.4) and 10 mM $CaCl_2$. Thereafter, gels were stained with Coomassie brilliant R-250 and destained in a solution of 7.5% acetic acid and 5% methanol. Zones of enzymatic activity appeared as clear bands against a blue background. The zone areas were measured using a computer image analysis system (Alpha Innotech Corporation; IS1000).

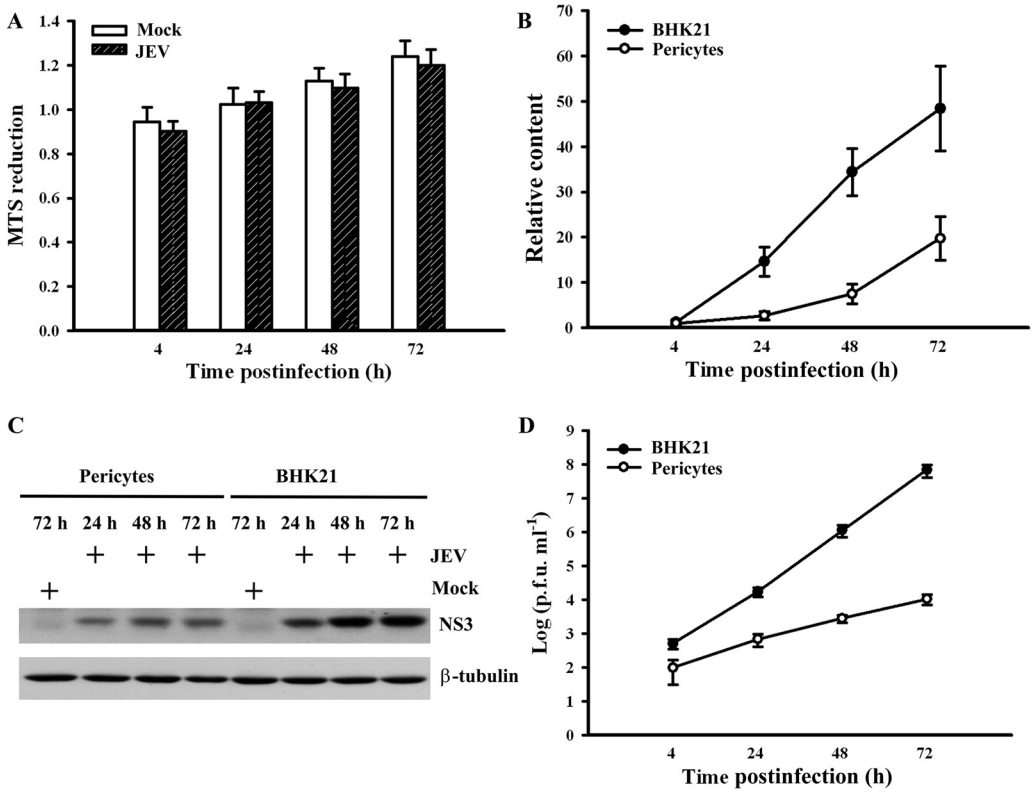

FIG 2 Characterization of JEV replication in pericytes. (A) Pericytes were mock infected or infected with JEV (MOI, 20) over time. Cell viability was measured by MTS reduction and expressed as arbitrary units. $n = 4$. Pericytes (MOI, 20) and BHK21 cells (MOI, 5) were mock infected or infected with JEV over time. (B) Total RNAs were isolated and subjected to quantitative real-time RT-PCR for the measurement of JEV genome and β-actin. Relative JEV genome content was determined by the $\Delta\Delta C_T$ method and expressed as arbitrary units. $n = 4$. (C) Total cellular proteins were isolated and subjected to Western blotting with antibodies against JEV NS3 and β-tubulin. Total cellular proteins obtained from mock-infected cells at the indicated times were used as a control. One representative blot of three independent experiments is shown. (D) The supernatants were collected and subjected to plaque assay for the determination of viral titers. $n = 4$.

Statistical analysis. The data are expressed as mean values ± standard deviations. Statistical analysis was carried out using one-way analysis of variance (ANOVA), followed by Dunnett's test to assess the statistical significance between treated and untreated groups in all experiments. A P value of <0.05 was considered statistically significant.

RESULTS

JEV-infected pericytes disrupted the integrity of endothelial barrier. Pericytes used in this study were prepared from the same brain microvascular vessels from which endothelial cells were obtained. Confluent monolayers of brain microvascular endothelial cells (Fig. 1A) and pericytes (Fig. 1B) obtained from adult Sprague-Dawley rats were examined under a light microscope. Phenotypic characteristics of endothelial cells were elucidated by the positivity of CD31 immunoreactivity (Fig. 1C, left graph) and the negativity of α-SMA immunoreactivity (Fig. 1C, right graph). Pericyte cultures were found to be negative for CD31 (Fig. 1D, left graph) and positive for α-SMA (Fig. 1D, right graph). More than 95% of cultured cells were identified to be endothelial cells and pericytes. Previously, we found that cultured brain microvascular endothelial cells were susceptible to JEV infection with limited amplification (25). As with endothelial cells, JEV infection had a negligible effect on the viability of pericytes (Fig. 2A). Although JEV (multiplicity of infection [MOI], 20) replicated in pericytes, the amplification of viral RNA (Fig. 2B), the expression of viral nonstructural protein NS3 (Fig. 2C), and the production of infectious virus particles (Fig. 2D) were not as elevated as those in BHK21 cells (MOI, 5). As a quantitative measurement of the impact of pericytes on the endothelial barrier integrity during the course of JEV infection, we monitored the TEER (Fig. 3, upper graphs) and permeability to dextran-FITC (Fig. 3, lower graphs) of the brain microvascular endothelial cell monoculture and the coculture of brain microvascular endothelial cells and pericytes. As shown in a previous report (25), JEV infection had negligible effects on the established electrical resistance and impermeability (Fig. 3A) in monoculture. When pericytes were grown over the established monolayers of endothelial cells, the endothelial barrier integrity was compromised in response to JEV infection (Fig. 3B). To further demonstrate the potential disrupting effect of pericytes on endothelial barrier integrity during JEV infection, coculture of monolayers of endothelial cells and pericytes was established by separation with a microporous Transwell filter insert. Infection of pericytes with JEV in the lower chambers also caused disruption of endothelial barrier integrity (Fig. 3C). This coculture enables the endothelial cells and pericytes to interact via soluble factors. To verify whether the barrier disruption consequence is mediated indirectly through soluble bioactive molecules released by JEV-infected pericytes, the supernatants from infected pericytes were collected. In comparison with mock-infected control, the exposure of endothelial cell monoculture with supernatants obtained from JEV-infected pericytes compromised endothelial barrier in-

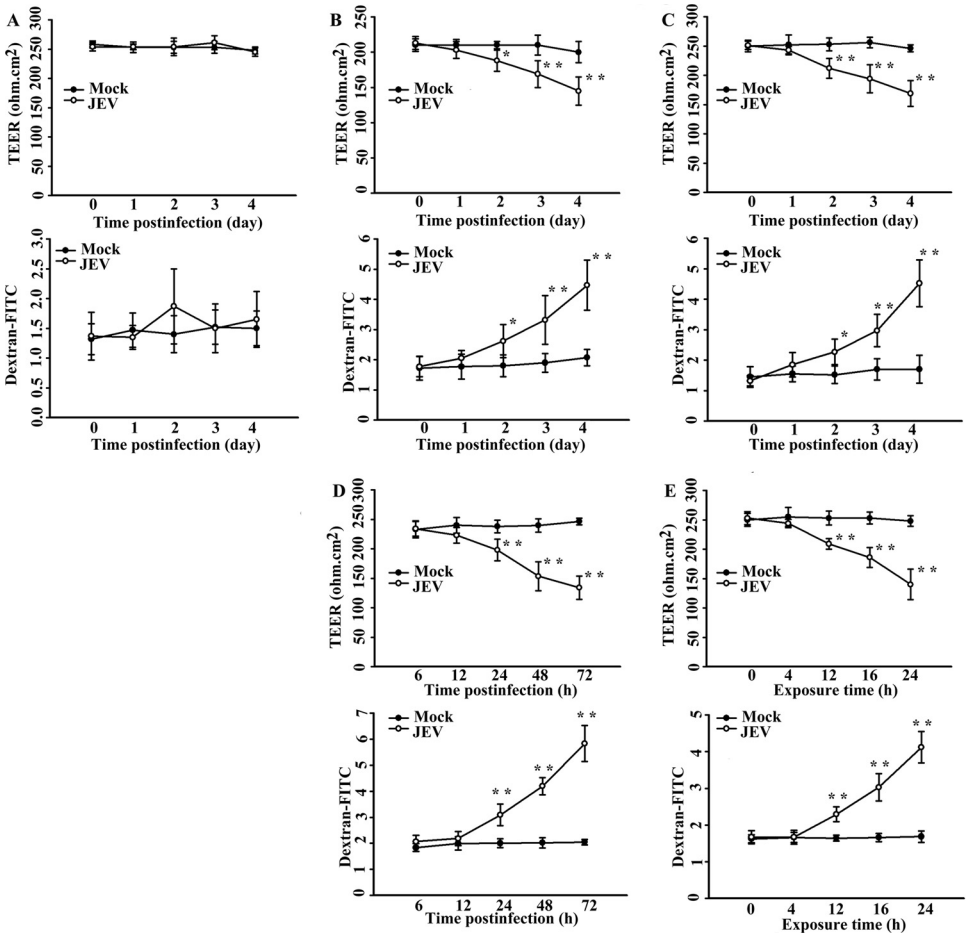

FIG 3 Effects of JEV infection on TEER and transendothelial permeability. (A) Confluent monolayers of brain microvascular endothelial cells were mock infected or infected with JEV (MOI, 20) over time. The TEER (upper graph) and transendothelial permeability to dextran-FITC (lower graph) were measured at the indicated times. The coculture of brain microvascular endothelial cells and pericytes seeded together (B) and separated by Transwell filter insert (C) was mock infected or infected with JEV (MOI, 20) over time. The TEER (upper graph) and transendothelial permeability to dextran-FITC (lower graph) were measured at the indicated times. (D) Pericytes were mock infected or infected with JEV (MOI, 20) over time. The supernatants were collected at the indicated times after infection and mixed with an equal volume of fresh medium. The manipulated media were added to brain microvascular endothelial cells for 24 h. The TEER (upper graph) and transendothelial permeability to dextran-FITC (lower graph) were measured. (E) Pericytes were mock infected or infected with JEV (MOI, 20) for 48 h. The supernatants were collected and mixed with an equal volume of fresh medium. The manipulated media were added to brain microvascular endothelial cells over time. The TEER (upper graph) and transendothelial permeability to dextran-FITC (lower graph) were measured at the indicated times. The values of TEER were given in ohm · cm^2 and the relative levels of dextran-FITC were expressed as arbitrary units. *, $P < 0.05$, and **, $P < 0.01$, versus each mock control; $n = 4$.

tegrity, and the disruption was apparently increased with the progression of infection (Fig. 3D). The supernatants collected from pericytes 48 h after JEV infection decreased TEER and increased permeability to dextran-FITC in endothelial cell monoculture, and remarkable disruption started to occur 12 h after exposure (Fig. 3E). These results suggest that pericyte-derived bioactively soluble molecules induced by JEV infection play a role in disrupting endothelial barrier integrity during the course of infection.

JEV-infected pericytes caused selective degradation of tight junction proteins. Since the expression and subcellular distribution of tight junction proteins such as claudin, occludin, and ZO play a key role in the physiology of endothelial barrier integrity (1, 2), we first examined their expression in endothelial cell monoculture after exposure to supernatants collected from pericytes 48 h after infection. The supernatants collected from pericytes 48 h after mock and JEV infection were mixed with equal volumes of fresh DMEM; these mixtures are referred to as mock-conditioned medium and JEV-conditioned medium, respectively, and they were used for the following experiments. The data of Western blotting revealed that the additions of JEV-conditioned medium to endothelial cells caused a reduction of endothelial ZO-1 protein ($P < 0.01$; $n = 4$). Unlike ZO-1, the protein levels of ZO-2, claudin-1, claudin-5, and occludin remained relatively constant (Fig. 4A). No remarkable difference in the levels of ZO-1 mRNA was detected (Fig. 4B). To examine whether the reduction seen in the total amounts of ZO-1 protein could be visualized by immunofluorescence staining, a set of immunofluorescence experiments was performed. In comparison with the mock control, an apparent reduction in the amounts of surface staining of ZO-1 was observed in cells exposed to JEV-conditioned medium. There was still no apparent difference in the amounts of surface staining of occludin between these two groups (Fig. 4C). The findings of these experi-

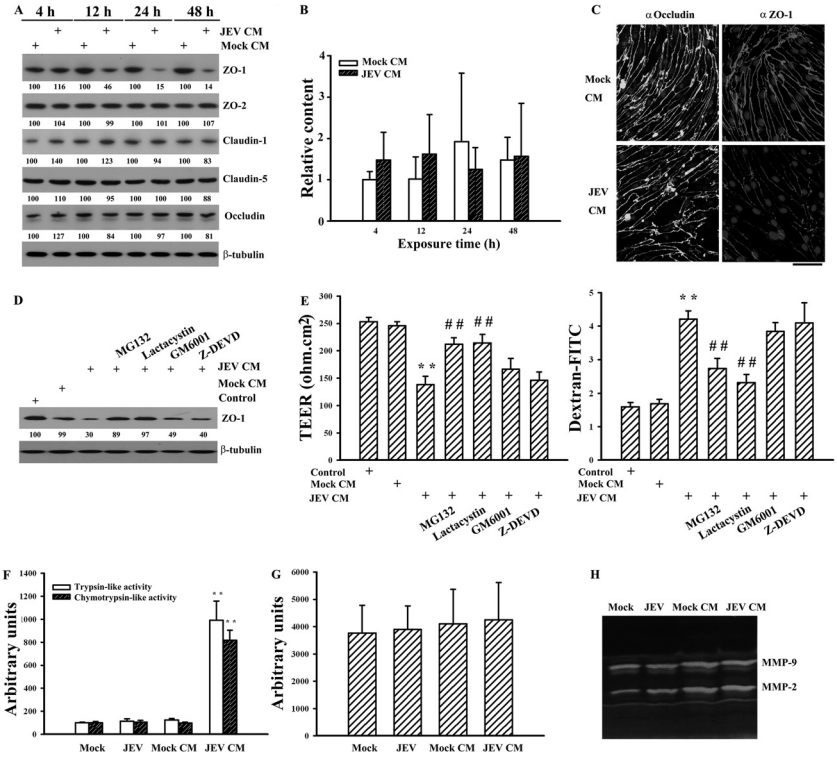

FIG 4 Effects on tight junction protein expression. Pericytes were mock infected (Mock CM) or infected with JEV (MOI, 20; JEV CM) for 48 h. The supernatants were collected and mixed with an equal volume of fresh medium. The manipulated media were added to brain microvascular endothelial cells over time. (A) Total cellular proteins were isolated and subjected to Western blotting with antibodies against ZO-1, ZO-2, claudin-1, claudin-5, occludin, and β-tubulin. One representative blot of four independent experiments is shown. The content in Mock CM at each time point was defined as 100%. (B) Total RNAs were isolated and subjected to quantitative real-time RT-PCR for the measurement of ZO-1 and β-actin. Relative gene expression was determined by the $\Delta\Delta C_T$ method, and the level in Mock CM at 4 h was defined as 1. $n = 4$. (C) The manipulated media (Mock CM and JEV CM) were added to brain microvascular endothelial cells for 24 h. The cells were subjected to immunofluorescence staining with antibodies against occludin (FITC) or ZO-1 (rhodamine) and counterstained with Hoechst 33342. The manipulated media (Mock CM and JEV CM) were added to brain microvascular endothelial cells in the absence or presence of MG132 (5 μM), lactacystin (50 μM), GM6001 (10 μM), or Z-DEVD (20 μM) for 24 h. Untreated cells were used as the control. (D) Total cellular proteins were isolated and subjected to Western blotting with antibodies against ZO-1 and β-tubulin. One representative blot of four independent experiments is shown. The content in control was defined as 100%. (E) The TEER (left graph) and transendothelial permeability to dextran-FITC (right graph) were measured. $n = 4$. Brain microvascular endothelial cells were mock infected or infected with JEV (MOI, 20) or exposed to the manipulated media (Mock CM and JEV CM) for 24 h. (F) Cellular proteins were isolated and subjected to fluorogenic assay for the determinations of trypsin-like and chemotrypsin-like proteasome activities. $n = 4$. (G) Cellular proteins were isolated and subjected to fluorogenic assay for the determination of caspase-3 activity. $n = 4$. (H) The supernatants were collected and subjected to zymography for determination of MMP-2 and MMP-9 activities. One representative blot of four independent experiments is shown. **, $P < 0.01$ versus Mock CM; ##, $P < 0.01$ versus JEV CM.

ments suggest that a protein degradation mechanism might be involved in the ZO-1 protein reduction seen in this study. Thus, the potential involvement of proteases was evaluated by addition of pharmacological inhibitors to endothelial cells during exposure periods. As shown in Fig. 4D, inhibition of ubiquitin-proteasome activity by MG132 ($P < 0.01$, $n = 4$) and lactacystin ($P < 0.01$, $n = 4$) attenuated JEV-conditioned medium-induced ZO-1 degradation. However, this reversal was not observed by inhibiting metalloproteinase activity (GM6001) or caspase-3 activity (Z-DEVD). Parallel studies also showed that only MG132 and lactacystin alleviated JEV-conditioned medium-induced endothelial barrier disruption (Fig. 4E). To further verify the potential involvement of proteases, endothelial proteasome, caspase, and metalloproteinase activities were measured. No apparent difference in proteasome activity was detected in endothelial cells directly mock infected or infected with JEV or exposed to mock-conditioned medium (Fig. 4F). However, the exposure of JEV-conditioned medium increased trypsin-like and chymotrypsin-like proteasome activities (Fig. 4F). There was no remarkable difference in activity of caspase-3 (Fig. 4G) or metalloproteinase (Fig. 4H) among the groups. These results suggest that the activation of endothelial ubiquitin-proteasome activity and consequent ZO-1 degradation might play an active role in endothelial barrier disruption caused by JEV-infected pericytes.

JEV infection induced expression of IL-6 and contributed to barrier disruption. There is evidence showing that microvascular endothelial cells exposed to TNF-α, IL-1β, IL-6, or VEGF have increased paracellular permeability (30, 31). We assessed whether JEV infection induces pericytes to express elevated levels of cytokines, which participate in endothelial barrier disruption. Our results showed that wild-type but not heat-inactivated JEV or mock infection caused robust IL-6 release from pericytes (Fig. 5A). In contrast, there was no remarkable production of TNF-α (Fig. 5B), IL-1β (Fig. 5C), and VEGF (Fig. 5D) during the course of JEV infection. To elucidate whether IL-6 plays a role in JEV-conditioned medium-induced permeability induction, the condi-

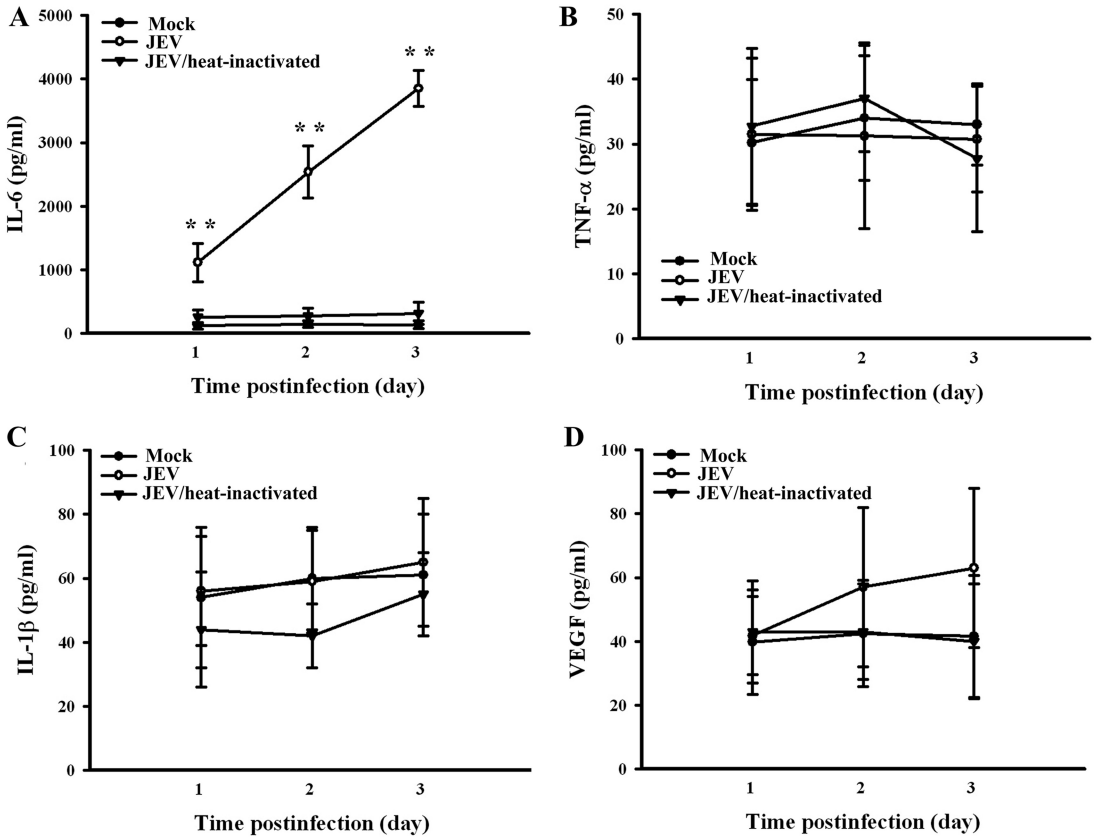

FIG 5 Effects on gene production. Pericytes were mock infected or infected with wild-type JEV (MOI, 20), or heat-inactivated JEV over time. Supernatants isolated from infected cells were subjected to ELISA for the measurement of IL-6 (A), TNF-α (B), IL-1β (C), and VEGF (D). **, $P < 0.01$ versus each mock control. $n = 4$.

tioned media were pretreated with IL-6 neutralizing antibody. Pretreatment with IL-6 neutralizing antibody had an inhibitory effect on JEV-conditioned medium-induced trypsin-like (Fig. 6A, left graph) and chymotrypsin-like (Fig. 6A, right graph) proteasome activation, ZO-1 protein reduction ($P < 0.05$; $n = 4$) (Fig. 6B), and endothelial barrier disruption (Fig. 6C). In parallel, the addition of exogenous IL-6 caused activation of trypsin-like (Fig. 6A, left graph) and chymotrypsin-like (Fig. 6A, right graph) proteasome activities, reduction of ZO-1 protein ($P < 0.01$; $n = 4$) (Fig. 6B), and disruption of endothelial barrier integrity (Fig. 6C) in monoculture of endothelial cells. Another set of experiments further showed that the production of IL-6 (Fig. 7A) and the disruption of endothelial barrier integrity (Fig. 7B) were positively correlated with infectious virus doses. Evidence suggests that the activation of Janus kinase (Jak)/signal transducers and activators of transcription (STAT) plays an important role in the signal transduction cascade event after the engagement of IL-6 and that its action can be blocked by pharmacological inhibitor AG490 (32). The results showed that AG490 was able to inhibit JEV-conditioned medium- and IL-6-induced trypsin-like (Fig. 6A, left panel) and chymotrypsin-like (Fig. 6A, right graph) proteasome activation, ZO-1 protein reduction ($P < 0.01$; $n = 4$) (Fig. 6B), and endothelial barrier disruption (Fig. 6C). These results suggest that IL-6 is crucial in triggering proteasomal degradation of ZO-1 and disruption of endothelial barrier integrity and that the pericytes actively produce IL-6 during JEV infection.

Upregulation of ubiquitin E3 ligase contributed to barrier disruption. E3 ubiquitin ligases play a crucial role and determine the substrate specificity in ubiquitin-proteasome degradation machinery. The activation of IL-6 signaling has been demonstrated to induce Ubr 1 expression, one E3 ubiquitin ligase (32–34). To elucidate the upstream regulatory mechanism of proteasomal degradation of ZO-1, the expression of Ubr 1 was examined. The results of Western blotting showed that the additions of JEV-conditioned medium to endothelial cells induced endothelial Ubr 1 expression (Fig. 8A) and that the elevation was attenuated by the pretreatment of IL-6 neutralizing antibody ($P < 0.01$; $n = 4$) or the addition of AG490 ($P < 0.01$; $n = 4$) (Fig. 8B). The potential involvement of elevated Ubr 1 in mediating the accompanying ZO-1 degradation and endothelial barrier disruption was evaluated by silencing Ubr 1 expression in endothelial cells before conditioned medium or IL-6 treatments. In comparison with scrambled control, the silencing of the Ubr 1 gene made endothelial cells more refractory to JEV-conditioned medium- and IL-6-induced Ubr 1 upregulation ($P < 0.01$; $n = 4$) as well as ZO-1 reduction ($P < 0.01$, $n = 4$) (Fig. 8C), trypsin-like (Fig. 8D, upper graph) and chymotrypsin-like (Fig. 8D, lower graph) proteasome activation, and barrier disruption (Fig. 8E). These results suggest that Ubr 1 is an active E3 ubiquitin ligase involved in triggering proteasomal degradation of ZO-1 and consequent disruption of endothelial barrier integrity in response to JEV-conditioned medium or IL-6 treatments.

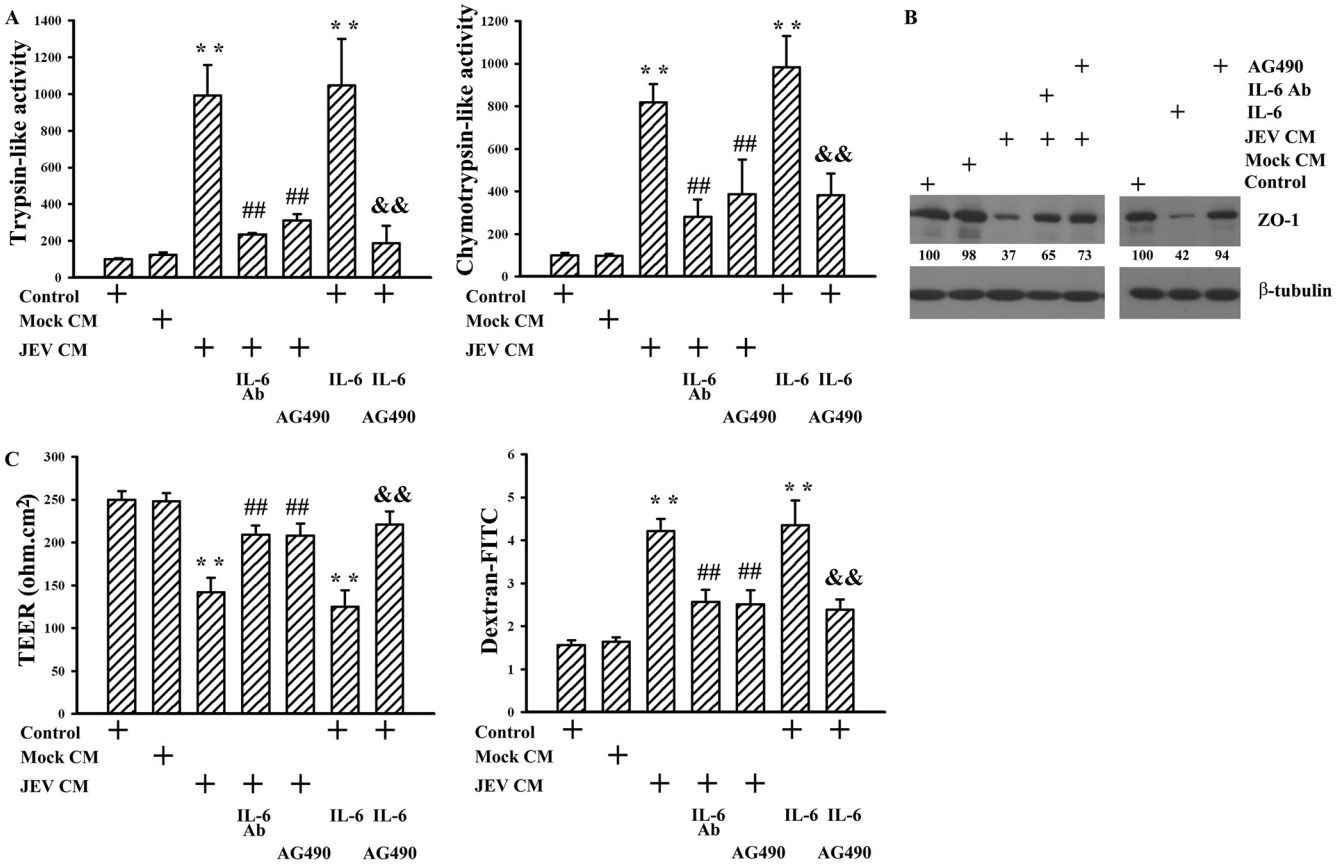

FIG 6 Role of IL-6. Pericytes were mock infected (Mock CM) or infected with JEV (MOI, 20; JEV CM) for 48 h. The supernatants were collected and mixed with an equal volume of fresh medium. Brain microvascular endothelial cells were exposed to the manipulated media (Mock CM and JEV CM) or treated with IL-6 (20 ng/ml) in the absence or presence of AG490 (50 μM) for 24 h. One set of manipulated medium (JEV CM) was modified by neutralization with IL-6 neutralizing antibody (10 μg/ml) for 30 min before being subjected to exposure. Untreated cells were used as the control. (A) Cellular proteins were isolated and subjected to fluorogenic assay for the determinations of trypsin-like (left graph) and chemotrypsin-like (right graph) proteasome activity. $n = 4$. (B) Total cellular proteins were isolated and subjected to Western blotting with antibodies against ZO-1 and β-tubulin. One representative blot of four independent experiments is shown. The content in control was defined as 100%. (C) The TEER (left graph) and transendothelial permeability to dextran-FITC (right graph) were measured. $n = 4$. **, $P < 0.01$ versus medium control; ##, $P < 0.01$ versus JEV CM; &&, $P < 0.01$ versus IL-6 control.

DISCUSSION

JEV-associated neurotoxicity, characterized by neuronal dysfunction and neuroinflammation, has been well demonstrated in clinical and animal studies. Peripheral JEV infection ultimately results in central neurodegeneration by a mechanism that is not yet fully understood, but it is known that the structural and functional integrity of the BBB is severely compromised and that these alterations have impacts on the development of Japanese encephalitis (15). Currently, there are few data on the relative contributions of the specific BBB cell types and mechanisms underlying the disruption of endothelial barrier integrity in Japanese encephalitis. Our previous study showed that direct infection of endothelial cells with JEV is not the determining event in regulating endothelial viability and barrier activity. Instead, JEV infection switches endothelial cells to the proinflammatory phenotype, which promotes recruitment of leukocytes and adhesion (25). Here, we showed that brain pericytes, another cell type of the BBB component, can be a target for JEV infection and plays a role in a mechanism which contributes to the disruption of endothelial barrier integrity. In comparison with monoculture of endothelial cells, coculture with pericytes, either in cell-cell contact or out of contact, caused proteasomal degradation of endothelial tight junction protein ZO-1 and decreased the tightness of endothelial monolayers in response to JEV infection. JEV infection of pericytes induced robust production of IL-6, and its elevation in the cultured supernatants correlated well with barrier disruption ability. In parallel with the activation of IL-6 signaling after exposure to JEV-conditioned medium, endothelial cells upregulated E3 ubiquitin ligase Ubr 1 expression, leading to proteasomal degradation of ZO-1 and causing disruption of endothelial barrier integrity. The findings from the relevant studies described above suggest a potential indirect mechanism in Japanese encephalitis-associated BBB breakdown involving pericytes.

The formation and maintenance of BBB integrity depend critically on the interaction of endothelial cells with other cell types of the neurovascular unit. Therefore, cell culture-based *in vitro* BBB models have been developed using monoculture of brain microvascular endothelial cells or coculture of brain microvascular endothelial cells with other BBB component cells (35). In this study, monoculture of endothelial cells and coculture of endothelial cells with pericytes in a direct contact manner orchestrated functional barrier integrity as evidenced by the establishment of electrical

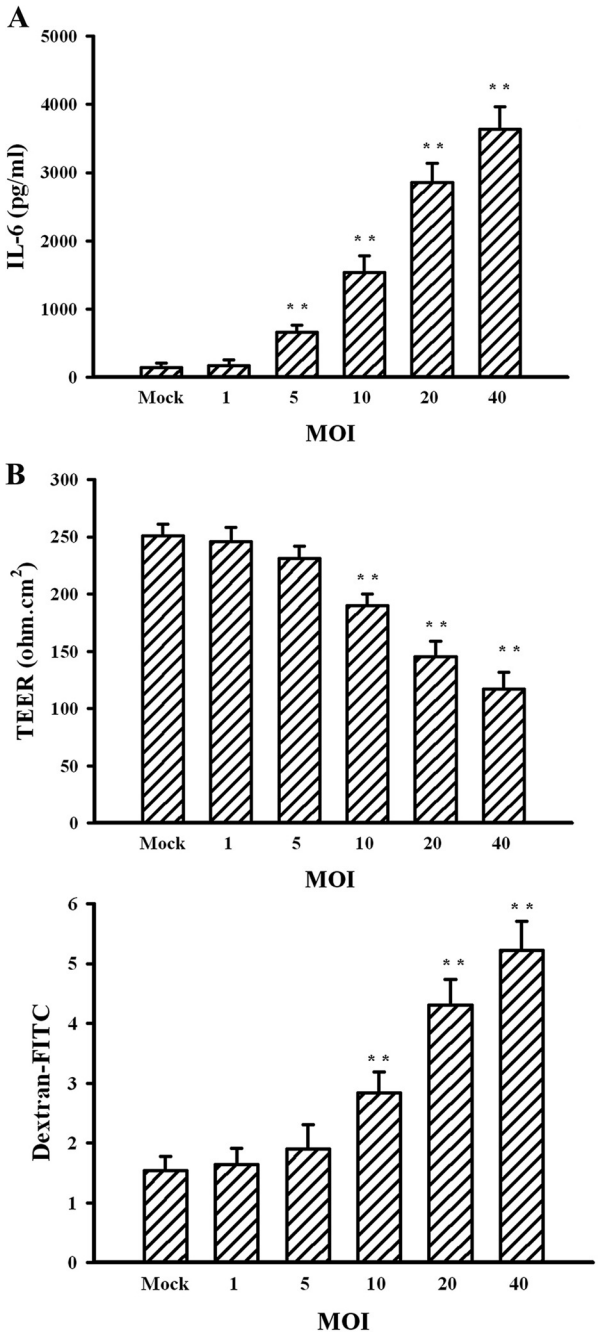

FIG 7 Effects of JEV infection on IL-6 expression. Pericytes were mock infected or infected with JEV (MOIs, 1, 5, 10, 20, and 40) for 48 h. (A) Supernatants isolated from infected cells were subjected to ELISA for the measurement of IL-6. $n = 4$. (B) The supernatants were collected and mixed with an equal volume of fresh medium. The manipulated media were added to brain microvascular endothelial cells for 24 h. The TEER (upper graph) and transendothelial permeability to dextran-FITC (lower graph) were measured. $n = 4$. **, $P < 0.01$ versus mock.

resistance and impermeability, particularly the former. Both endothelial cells (25) and pericytes were susceptible to JEV infection but with a limited efficacy and a negligible cytotoxicity under experimental conditions compared with BHK21 cell line. The significance of JEV-induced endothelial barrier disruption was observed in *in vitro* coculture but not in a monoculture model. Increasing evidence demonstrates the specific role and contribution of endothelial cells, astrocytes, and pericytes in neurotropic virus-associated BBB breakdown (6, 23, 24, 28, 36). In a Japanese encephalitis animal model, electron microscopic examination revealed the presence of virions in BBB-associated endothelial cells and pericytes (16, 17), suggesting the potential involvement of endothelial cells or pericytes in accompanying BBB breakdown. Although pericytes possess permeability-inducing and -reducing effects (19, 20), we found that pericytes acquired barrier disruption ability in response to JEV infection. A similar permeability-inducing effect was demonstrated in pericytes infected with human immunodeficiency virus type 1 (HIV-1) (23). Thus, our current findings suggest that the bystander effects from pericytes might play an active role in Japanese encephalitis-associated BBB breakdown.

The aforementioned results and those of relevant studies suggest that direct infection of endothelial cells with JEV has a negligible effect in regulating barrier activity. Other events such as cell-cell interaction and soluble-molecule bioactivity might be involved. The results of coculture with separated cell layers and exposure to conditioned medium further emphasize the crucial role of biologically active molecules released by JEV-infected pericytes. The regulation of BBB integrity by pericytes is of increasing interest due to the fact that these cells are in close proximity to brain endothelium and release a large number of endothelial permeability-regulating molecules. Pericytes are known to secrete elevated levels of permeability-inducing factors such as TNF-α, IL-1β, IL-6, metalloproteinases, and VEGF under different conditions (19–22, 24). These factors were elevated in JEV-infected animals and cultured glial cells (10, 11, 15, 31, 37–39). However, in this experimental model, there was no apparent induction of TNF-α, IL-1β, VEGF, or metalloproteinases and only induction of IL-6 in JEV-infected pericytes. During JEV infection, the permeability-inducing effect of IL-6 was supported by the finding of the inhibitory effect of IL-6 neutralizing antibody against JEV-conditioned medium-induced barrier disruption and the barrier-disrupting effect of exogenous recombinant IL-6. The corresponding compromised endothelial barrier integrity by infected pericytes and accompanying IL-6 production was also noted in cases of HIV-1 and human cytomegalovirus infection (22, 23). In addition to macrophage-derived neutrophil chemotactic factor (15), our findings suggest that IL-6 released by brain microvascular endothelium neighboring pericytes is of paramount importance in Japanese encephalitis-associated BBB breakdown.

Breakdown of the BBB has been previously demonstrated in JEV-infected animals. The demise of endothelial cells and/or the degradation or dissociation of tight junction proteins can in most cases be attributed to BBB disruption (10, 15–18). Tight junction proteins, including occludin and claudins that are joined to the cytoskeleton by the cytoplasmic proteins, such as ZOs in particular, play a key role in restricting paracellular permeability. The events of their transcription, translation, degradation, phosphorylation, and subcellular distribution control the formation and activity of tight junctions. Of particular importance are the matrix metalloproteinases, which are a protease family crucial to the degradation of tight junction proteins. The activation of metalloproteinases causes a degradation of tight junction proteins, including ZO-1, leading to the disruption of barrier integrity (1, 2, 28, 36, 40, 41). However, metalloproteinases seemed to play a negligible

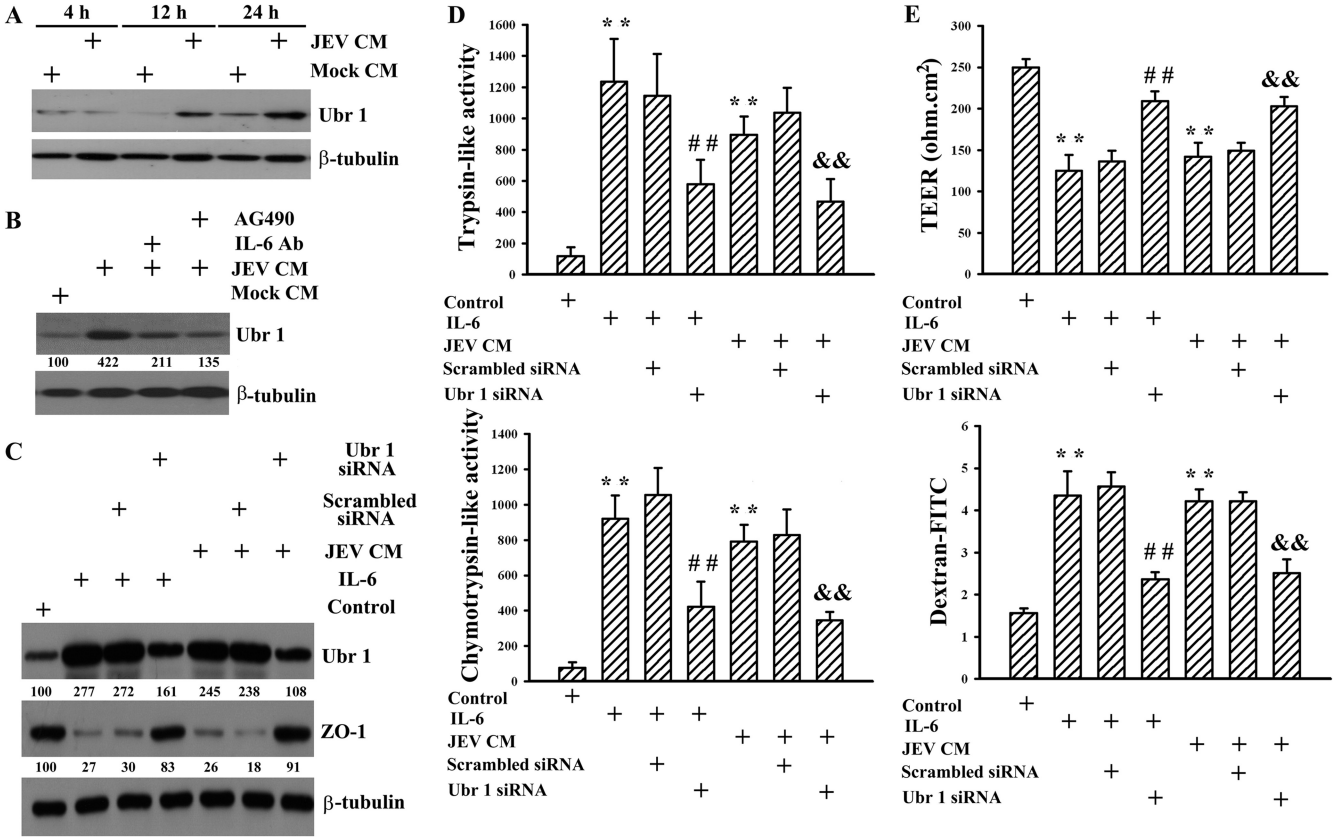

FIG 8 Role of Ubr 1. Pericytes were mock infected (Mock CM) or infected with JEV (MOI, 20; JEV CM) for 48 h. The supernatants were collected and mixed with an equal volume of fresh medium. (A) The manipulated media were added to brain microvascular endothelial cells over time. Total cellular proteins were isolated and subjected to Western blotting with antibodies against Ubr 1 and β-tubulin. One representative blot of four independent experiments is shown. (B) Brain microvascular endothelial cells were exposed to the manipulated media (Mock CM and JEV CM) in the absence or presence of AG490 (50 μM) for 24 h. One set of manipulated medium (JEV CM) was modified by neutralization with IL-6 neutralizing antibody (10 μg/ml) for 30 min before being subjected to exposure. Total cellular proteins were isolated and subjected to Western blotting with antibodies against Ubr 1 and β-tubulin. One representative blot of four independent experiments is shown. The content in Mock CM was defined as 100%. Brain microvascular endothelial cells were transfected with control siRNA (1 nM) (mock transfection) or Ubr 1 siRNA (1 nM) for 4 h. The resultant cells were treated with IL-6 (20 ng/ml) or exposed to JEV CM for 24 h. Untreated cells were used as a control. (C) Total cellular proteins were isolated and subjected to Western blotting with antibodies against Ubr 1, ZO-1, and β-tubulin. One representative blot of four independent experiments is shown. The content in control was defined as 100%. (D) Cellular proteins were isolated and subjected to fluorogenic assay for determination of trypsin-like (upper graph) and chemotrypsin-like (lower graph) proteasome activities. $n = 4$. **, $P < 0.01$ versus medium control; ##, $P < 0.01$ versus IL-6 control; &&, $P < 0.01$ versus JEV CM control.

role in JEV-infected pericyte-induced barrier disruption. No apparent induction of metalloproteinase activity was detected in endothelial cells infected with JEV and exposed to JEV-conditioned medium. An elevated expression of metalloproteinase was demonstrated in rat astrocytes in response to JEV infection (42). That is, despite the crucial role of metalloproteinases in endothelial barrier integrity, their inductive expression varies and depends on cell types, stress, and microenviroments. Despite the successful detection of ZO-1, ZO-2, claudin-1, claudin-5, and occludin in our cultured endothelial cells, our data clearly showed an association between proteasomal degradation of ZO-1 and JEV-infected pericyte-induced disruption of endothelial barrier integrity. The degradation of ZO-1 and its reduction of surface presentation were accompanied by elevated proteasome activity in compromised endothelial cells. Other interesting findings in this study were that IL-6 participated in E3 ubiquitin ligase Ubr 1 expression and the consequent activation of ubiquitin proteasome and degradation of ZO-1 in brain microvascular endothelial cells. E3 ubiquitin ligases such as Itch and Nedd4 are involved in the proteasomal degradation of cytoplasmic proteins, including occludin (43, 44). Evidence suggests that the expression of Ubr 1 is dependent on the STAT activity induced by the IL-6/gp130 signaling pathway (32, 45). By extending the scope of these studies, we have demonstrated that the expression of Ubr 1 via stimulation with IL-6 is an alternative regulatory mechanism of cytoplasmic ZO-1 degradation. The presence of elevated levels of IL-6, activation of the STAT pathway, deformation of tight junctions, and disruption of the BBB have been observed in a mouse model of Japanese encephalitis (10, 15–18, 38, 39). The results of this *in vitro* study showed parallel changes and demonstrated their execution and potential cross talk in endothelial cells and pericytes during the course of JEV infection. It should be noted that astrocytes and microglia are also capable of inducing IL-6 expression in response to JEV infection (37). Therefore, the cross talk between endothelial cells and other cells such as as-

trocytes and microglia through IL-6 was highly expected but not addressed in current study.

Brain homeostasis is maintained by the structure and function of the BBB, which plays a key role in the pathogenesis of neurotropic viruses by regulating the entry of circulating molecules, immune cells, or viruses into the CNS. Endothelial cells, which line the intraluminal portion of brain capillaries in close contact with basement membrane-embedded pericytes, are the direct targets of blood-borne materials. Previously, we found that JEV infection could activate brain microvascular endothelial cells and modify their proinflammatory characteristics without compromising the barrier integrity (25). In this study, we showed a potential mechanism of disruption of endothelial barrier integrity during the course of JEV infection through the activation of neighboring pericytes. JEV infection selectively triggers pericyte release of IL-6. Under pathophysiological conditions, the consequences of the released IL-6 are to turn on gene expression and induce proinflammatory responses. Our data demonstrate that IL-6 released by JEV-infected pericytes is critical for proteasomal degradation of ZO-1 and the accompanying disruption of endothelial barrier integrity through the induction of Ubr 1 in brain microvascular endothelial cells. Our findings show that pericytes can be a target for JEV infection and appear to be one of the mechanisms by which the integrity of endothelial barrier is compromised. Collectively, these data suggest that JEV infection could activate pericytes and release IL-6, thereby contributing, in concert with other unidentified barrier-disrupting factors, to the induction of Japanese encephalitis-associated BBB breakdown.

ACKNOWLEDGMENTS

This work was supported by grants from the National Science Council (NSC100-2314-B-075A-004 and NSC101-2314-B-075A-007) and a joint grant from Taichung Veterans General Hospital and Central Taiwan University of Sciences and Technology (TCVGH-CTUST987701), Taiwan.

The authors have no conflicts of interest to declare.

REFERENCES

1. **Hawkins BT, Davis TP.** 2005. The blood-brain barrier/neurovascular unit in health and disease. Pharmacol. Rev. **57:**173–185. http://dx.doi.org/10.1124/pr.57.2.4.
2. **Persidsky Y, Ramirez SH, Haorah J, Kanmogne GD.** 2006. Blood-brain barrier: structural components and function under physiologic and pathologic conditions. J. Neuroimmune Pharmacol. **1:**223–236. http://dx.doi.org/10.1007/s11481-006-9025-3.
3. **Afonso PV, Ozden S, Cumont MC, Seilhean D, Cartier L, Rezaie P, Mason S, Lambert S, Huerre M, Gessain A, Couraud PO, Pique C, Ceccaldi PE, Romero IA.** 2008. Alteration of blood-brain barrier integrity by retroviral infection. PLoS Pathog. **4:**e1000205. http://dx.doi.org/10.1371/journal.ppat.1000205.
4. **Chaturvedi UC, Dhawan R, Khanna M, Mathur A.** 1991. Breakdown of the blood-brain barrier during dengue virus infection of mice. J. Gen. Virol. **72:**859–866. http://dx.doi.org/10.1099/0022-1317-72-4-859.
5. **Schäfer A, Brooke CB, Whitmore AC, Johnston RE.** 2011. The role of the blood-brain barrier during Venezuelan equine encephalitis virus infection. J. Virol. **85:**10682–10690. http://dx.doi.org/10.1128/JVI.05032-11.
6. **Soilu-Hänninen M, Erälinna JP, Hukkanen V, Röyttä M, Salmi AA, Salonen R.** 1994. Semliki Forest virus infects mouse brain endothelial cells and causes blood-brain barrier damage. J. Virol. **68:**6291–6298.
7. **Roy A, Hooper DC.** 2007. Lethal silver-haired bat rabies virus infection can be prevented by opening the blood-brain barrier. J. Virol. **81:**7993–7998. http://dx.doi.org/10.1128/JVI.00710-07.
8. **Chambers TJ, Hahn CS, Galler R, Rice CM.** 1990. Flavivirus genome organization, expression, and replication. Annu. Rev. Microbiol. **44:**649–688. http://dx.doi.org/10.1146/annurev.mi.44.100190.003245.
9. **Solomon T, Dung NM, Kneen R, Gainsborough M, Vaughn DW, Khanh VT.** 2000. Japanese encephalitis. J. Neurol. Neurosurg. Psychiatry **68:**405–415. http://dx.doi.org/10.1136/jnnp.68.4.405.
10. **German AC, Myint KS, Mai NT, Pomeroy I, Phu NH, Tzartos J, Winter P, Collett J, Farrar J, Barrett A, Kipar A, Esiri MM, Solomon T.** 2006. A preliminary neuropathological study of Japanese encephalitis in humans and a mouse model. Trans. R. Soc. Trop. Med. Hyg. **100:**1135–1145. http://dx.doi.org/10.1016/j.trstmh.2006.02.008.
11. **Ghoshal A, Das S, Ghosh S, Mishra MK, Sharma V, Koli P, Sen E, Basu A.** 2007. Proinflammatory mediators released by activated microglia induce neuronal death in Japanese encephalitis. Glia **55:**483–496. http://dx.doi.org/10.1002/glia.20474.
12. **Ravi V, Parida S, Desai A, Chandramuki A, Gourie-Devi M, Grau GE.** 1997. Correlation of tumor necrosis factor levels in the serum and cerebrospinal fluid with clinical outcome in Japanese encephalitis patients. J. Med. Virol. **51:**132–136. http://dx.doi.org/10.1002/(SICI)1096-9071(199702)51:2<132::AID-JMV8>3.0.CO;2-8.
13. **Winter PM, Dung NM, Loan HT, Kneen R, Wills B, Thu le T, House D, White NJ, Farrar JJ, Hart CA, Solomon T.** 2004. Proinflammatory cytokines and chemokines in humans with Japanese encephalitis. J. Infect. Dis. **190:**1618–1626. http://dx.doi.org/10.1086/423328.
14. **Saxena V, Mathur A, Krishnani N, Dhole TN.** 2008. Kinetics of cytokine profile during intraperitoneal inoculation of Japanese encephalitis virus in BALB/c mice model. Microbes Infect. **10:**1210–1217. http://dx.doi.org/10.1016/j.micinf.2008.06.015.
15. **Mathur A, Khanna N, Chaturvedi UC.** 1992. Breakdown of blood-brain barrier by virus-induced cytokine during Japanese encephalitis virus infection. Int. J. Exp. Pathol. **73:**603–611.
16. **Liu TH, Liang LC, Wang CC, Liu HC, Chen WJ.** 2008. The blood-brain barrier in the cerebrum is the initial site for the Japanese encephalitis virus entering the central nervous system. J. Neurovirol. **14:**514–521. http://dx.doi.org/10.1080/13550280802339643.
17. **Liou ML, Hsu CY.** 1998. Japanese encephalitis virus is transported across the cerebral blood vessels by endocytosis in mouse brain. Cell Tissue Res. **293:**389–394. http://dx.doi.org/10.1007/s004410051130.
18. **Mishra MK, Dutta K, Saheb SK, Basu A.** 2009. Understanding the molecular mechanism of blood-brain barrier damage in an experimental model of Japanese encephalitis: correlation with minocycline administration as a therapeutic agent. Neurochem. Int. **55:**717–723. http://dx.doi.org/10.1016/j.neuint.2009.07.006.
19. **Nakagawa S, Deli MA, Nakao S, Honda M, Hayashi K, Nakaoke R, Kataoka Y, Niwa M.** 2007. Pericytes from brain microvessels strengthen the barrier integrity in primary cultures of rat brain endothelial cells. Cell. Mol. Neurobiol. **27:**687–694. http://dx.doi.org/10.1007/s10571-007-9195-4.
20. **Thanabalasundaram G, Pieper C, Lischper M, Galla HJ.** 2010. Regulation of the blood-brain barrier integrity by pericytes via matrix metalloproteinases mediated activation of vascular endothelial growth factor in vitro. Brain Res. **1347:**1–10. http://dx.doi.org/10.1016/j.brainres.2010.05.096.
21. **Thanabalasundaram G, Schneidewind J, Pieper C, Galla HJ.** 2011. The impact of pericytes on the blood-brain barrier integrity depends critically on the pericyte differentiation stage. Int. J. Biochem. Cell Biol. **43:**1284–1293. http://dx.doi.org/10.1016/j.biocel.2011.05.002.
22. **Alcendor DJ, Charest AM, Zhu WQ, Vigil HE, Knobel SM.** 2012. Infection and upregulation of proinflammatory cytokines in human brain vascular pericytes by human cytomegalovirus. J. Neuroinflamm. **9:**95. http://dx.doi.org/10.1186/1742-2094-9-95.
23. **Nakagawa S, Castro V, Toborek M.** 2012. Infection of human pericytes by HIV-1 disrupts the integrity of the blood-brain barrier. J. Cell. Mol. Med. **16:**2950–2957. http://dx.doi.org/10.1111/j.1582-4934.2012.01622.x.
24. **Vandenhaute E, Culot M, Gosselet F, Dehouck L, Godfraind C, Franck M, Plouët J, Cecchelli R, Dehouck MP, Ruchoux MM.** 2012. Brain pericytes from stress-susceptible pigs increase blood-brain barrier permeability in vitro. Fluids Barriers CNS **9:**11. http://dx.doi.org/10.1186/2045-8118-9-11.
25. **Lai CY, Ou YC, Chang CY, Pan HC, Chang CJ, Liao SL, Su HL, Chen CJ.** 2012. Endothelial Japanese encephalitis virus infection enhances migration and adhesion of leukocytes to brain microvascular endothelia via MEK-dependent expression of ICAM1 and the CINC and RANTES chemokines. J. Neurochem. **123:**250–261. http://dx.doi.org/10.1111/j.1471-4159.2012.07889.x.
26. **András IE, Pu H, Deli MA, Nath A, Hennig B, Toborek M.** 2003. HIV-1 Tat protein alters tight junction protein expression and distribution in

cultured brain endothelial cells. J. Neurosci. Res. **74:**255–265. http://dx.doi.org/10.1002/jnr.10762.
27. **Tedelind S, Ericson LE, Karlsson JO, Nilsson M.** 2003. Interferon-γ down-regulates claudin-1 and impairs the epithelial barrier function in primary cultured human thyrocytes. Eur. J. Endocrinol. **149:**215–221. http://dx.doi.org/10.1530/eje.0.1490215.
28. **Xu R, Feng X, Xie X, Zhang J, Wu D, Xu L.** 2012. HIV-1 Tat protein increases the permeability of brain endothelial cells by both inhibiting occludin expression and cleaving occludin via metalloproteinase-9. Brain Res. **1436:**13–19. http://dx.doi.org/10.1016/j.brainres.2011.11.052.
29. **Wang YY, Chen CJ, Lin SY, Chuang YH, Sheu WH, Tung KC.** 2013. Hyperglycemia is associated with enhanced gluconeogenesis in a rat model of permanent cerebral ischemia. Mol. Cell. Endocrinol. **367:**50–56. http://dx.doi.org/10.1016/j.mce.2012.12.016.
30. **Candelario-Jalil E, Taheri S, Yang Y, Sood R, Grossetete M, Estrada EY, Fiebich BL, Rosenberg GA.** 2007. Cyclooxygenase inhibition limits blood-brain barrier disruption following intracerebral injection of tumor necrosis factor-alpha in the rat. J. Pharmacol. Exp. Ther. **323:**488–498. http://dx.doi.org/10.1124/jpet.107.127035.
31. **de Vries HE, Blom-Roosemalen MC, van Oosten M, de Boer AG, van Berkel TJ, Breimer DD, Kuiper J.** 1996. The influence of cytokines on the integrity of the blood-brain barrier in vitro. J. Neuroimmunol. **64:**37–43. http://dx.doi.org/10.1016/0165-5728(95)00148-4.
32. **Ozawa Y, Nakao K, Kurihara T, Shimazaki T, Shimmura S, Ishida S, Yoshimura A, Tsubota K, Okano H.** 2008. Roles of STAT3/SOCS3 pathway in regulating the visual function and ubiquitin-proteasome-dependent degradation of rhodopsin during retinal inflammation. J. Biol. Chem. **283:**24561–24570. http://dx.doi.org/10.1074/jbc.M802238200.
33. **Eisele F, Wolf DH.** 2008. Degradation of misfolded protein in the cytoplasm is mediated by the ubiquitin ligase Ubr 1. FEBS Lett. **582:**4143–4146. http://dx.doi.org/10.1016/j.febslet.2008.11.015.
34. **Heck JW, Cheung SK, Hampton RY.** 2010. Cytoplasmic protein quality control degradation mediated by parallel actions of the E3 ubiquitin ligases Ubr1 and San1. Proc. Natl. Acad. Sci. U. S. A. **107:**1106–1111. http://dx.doi.org/10.1073/pnas.0910591107.
35. **Nakagawa S, Deli MA, Kawaguchi H, Shimizudani T, Shimono T, Kittel A, Tanaka K, Niwa M.** 2009. A new blood-brain barrier model using primary rat brain endothelial cells, pericytes, and astrocytes. Neurochem. Int. **54:**253–263. http://dx.doi.org/10.1016/j.neuint.2008.12.002.
36. **Verma S, Kumar M, Gurjav U, Lum S, Nerurkar VR.** 2010. Reversal of West Nile virus-induced blood-brain barrier disruption and tight junction proteins degradation by matrix metalloproteinase inhibitor. Virology **397:**130–138. http://dx.doi.org/10.1016/j.virol.2009.10.036.
37. **Chen CJ, Ou YC, Lin SY, Raung SL, Liao SL, Lai CY, Chen SY, Chen JH.** 2010. Glial activation involvement in neuronal death by Japanese encephalitis virus infection. J. Gen. Virol. **91:**1028–1037. http://dx.doi.org/10.1099/vir.0.013565-0.
38. **Gupta N, Rao PV.** 2011. Transcriptomic profile of host response in Japanese encephalitis virus infection. Virol. J. **8:**92. http://dx.doi.org/10.1186/1743-422X-8-92.
39. **Yang Y, Ye J, Yang X, Jiang R, Chen H, Cao S.** 2011. Japanese encephalitis virus infection induces changes of mRNA profile of mouse spleen and brain. Virol. J. **8:**80. http://dx.doi.org/10.1186/1743-422X-8-80.
40. **Xie H, Xue Y, Liu L, Liu Y.** 2010. Endothelial-monocyte-activating polypeptide II increases blood-brain barrier permeability by down-regulating the expression levels of tight junction associated proteins. Brain Res. **1319:**13–20. http://dx.doi.org/10.1016/j.brainres.2010.01.023.
41. **Yamamoto M, Ramirez SH, Sato S, Kiyota T, Cerny RL, Kaibuchi K, Persidsky Y, Ikezu T.** 2008. Phosphorylation of claudin-5 and occludin by Rho kinase in brain endothelial cells. Am. J. Pathol. **172:**521–533. http://dx.doi.org/10.2353/ajpath.2008.070076.
42. **Tung WH, Tsai HW, Lee IT, Hsieh HL, Chen WJ, Chen YL, Yang CM.** 2010. Japanese encephalitis virus induces matrix metalloproteinase-9 in rat brain astrocytes via NF-κB signaling dependent on MAPKs and reactive oxygen species. Br. J. Pharmacol. **161:**1566–1583. http://dx.doi.org/10.1111/j.1476-5381.2010.00982.x.
43. **Traweger A, Fang D, Liu YC, Stelzhammer W, Krizbai IA, Fresser F, Bauer HC, Bauer H.** 2002. The tight junction-specific protein occludin is a functional target of the E3 ubiquitin-protein ligase Itch. J. Biol. Chem. **277:**10201–10208. http://dx.doi.org/10.1074/jbc.M111384200.
44. **Wang C, An J, Zhang P, Xu C, Gao K, Wu D, Wang D, Yu H, Liu JO, Yu L.** 2012. The Nedd4-like ubiquitin E3 ligases target angiomotin/p130 to ubiquitin-dependent degradation. Biochem. J. **444:**279–289. http://dx.doi.org/10.1042/BJ20111983.
45. **Sasaki T, Kojima H, Kishimoto R, Ikeda A, Kunimoto H, Nakajima K.** 2006. Spatiotemporal regulation of c-Fos by ERK5 and the E3 ubiquitin ligase UBR1, and its biological role. Mol. Cell **24:**63–75. http://dx.doi.org/10.1016/j.molcel.2006.08.005.